MOLECULAR AND CELLULAR BIOLOGY, June 2011, p. 2499–2512 Vol. 31, No. 12
0270-7306/11/$12.00 doi:10.1128/MCB.01046-10

Nonautonomous Apoptosis Is Triggered by Local Cell Cycle Progression during Epithelial Replacement in *Drosophila*▽†

Yu-ichiro Nakajima,[1] Erina Kuranaga,[1,2,3] Kaoru Sugimura,[4]‡ Atsushi Miyawaki,[4] and Masayuki Miura[1,2]*

Department of Genetics, Graduate School of Pharmaceutical Sciences, The University of Tokyo, 7-3-1 Hongo, Bunkyo-ku, Tokyo 113-0033, Japan[1]; Core Research for Evolutional Science and Technology (CREST), Japan Science and Technology Agency (JST), 7-3-1 Hongo, Bunkyo-ku, Tokyo 113-0033, Japan[2]; Laboratory for Histogenetic Dynamics, RIKEN Center for Developmental Biology, 2-2-3 Minatojima-minamimachi, Chuo-ku, Kobe 650-0047, Japan[3]; and Laboratory for Cell Function and Dynamics, Advanced Technology Development Group, Brain Science Institute, RIKEN, 2-1 Hirosawa, Wako-city, Saitama 351-0198, Japan[4]

Received 8 September 2010/Returned for modification 19 November 2010/Accepted 25 March 2011

Tissue remodeling involves collective cell movement, and cell proliferation and apoptosis are observed in both development and disease. Apoptosis and proliferation are considered to be closely correlated, but little is known about their coordinated regulation in physiological tissue remodeling *in vivo*. The replacement of larval abdominal epidermis with adult epithelium in *Drosophila* pupae is a simple model of tissue remodeling. During this process, larval epidermal cells (LECs) undergo apoptosis and are replaced by histoblasts, which are adult precursor cells. By analyzing caspase activation at the single-cell level in living pupae, we found that caspase activation in LECs is induced at the LEC/histoblast boundary, which expands as the LECs die. Manipulating histoblast proliferation at the LEC/histoblast boundary, either genetically or by UV illumination, indicated that local interactions with proliferating histoblasts triggered caspase activation in the boundary LECs. Finally, by monitoring the spatiotemporal dynamics of the S/G_2/M phase in histoblasts *in vivo*, we found that the transition from S/G_2 phases is necessary to induce nonautonomous LEC apoptosis at the LEC/histoblast boundary. The replacement boundary, formed as caspase activation is regulated locally by cell-cell communication, may drive the dynamic orchestration of cell replacement during tissue remodeling.

Tissue remodeling, whether in developmental or pathological contexts, involves collective cell behaviors, such as their formation into coherent groups or nests in which the cells are connected by cell-cell junctions, as they are in an epithelial sheet (13, 14). Although the dynamic rearrangement of cell populations requires collective migration and invasion, the individual cell behaviors, including cell proliferation, migration, cell shape changes, and cell death, are coordinated to accomplish this (39). In particular, cell death and cell proliferation, which are the fundamental features of net tissue growth during development and tissue homeostasis, must be coordinated (19).

Caspase-dependent cell death, or apoptosis, is an evolutionarily conserved mechanism (32), and it has been reported in tissue remodeling in several contexts. If a tissue is remodeled during development or accidentally injured, cell death (programmed or damage-induced) removes the cells, and their removal is offset by the proliferation of neighboring cells (53). Similarly, during regeneration, apoptosis signaling is essential for eliminating damaged tissue and for permitting new tissue to grow by stimulating proliferation in the surrounding cells (3, 8, 11, 20, 29, 54, 56, 66, 67). Wound healing also requires caspase activity for the maintenance of epidermal equilibrium (40). The remodeling process coupling apoptosis and proliferation is observed as well in cases of competition between cell populations, a phenomenon that was first described in a study of *Minute*/+ clones in developing *Drosophila* wings (44) and has been proposed to be related to cancer progression (45). In cell competition, tissue remodeling proceeds by coordinating proliferation and apoptosis between the faster-growing "winner" cells and the slower-growing "loser" cells. These findings suggest that the close correlation between apoptosis and proliferation is crucial for dynamic tissue remodeling that involves the replacement of cell populations without changing the total tissue size. However, the mechanisms governing the coupling of apoptosis and proliferation and the exact cellular events that take place *in vivo* remain poorly characterized.

The abdominal epithelial replacement in *Drosophila* is a suitable system for the detailed analysis of dynamic cell proliferation and apoptosis *in vivo*. In the pupal stage, the adult abdominal epidermis is formed by abdominal histoblasts, which replace the polyploid larval epidermal cells (LECs) (43). The histoblasts are born as a small group of cells and remain quiescent in lateral nests during the larval stages. These cells begin to divide upon pupariation. At about 15 h after puparium formation (APF), the nests expand, and the cells migrate collectively over the ventral and dorsal abdomen; during this migration, they replace the LECs, which undergo apoptosis at the same time (43).

During the abdominal epithelial replacement, the coordina-

* Corresponding author. Mailing address: Department of Genetics, Graduate School of Pharmaceutical Sciences, The University of Tokyo, 7-3-1 Hongo, Bunkyo-ku, Tokyo 113-0033, Japan. Phone: 81-3-5841-4860. Fax: 81-3-5841-4867. E-mail: miura@mol.f.u-tokyo.ac.jp.

† Supplemental material for this article may be found at http://mcb.asm.org/.

‡ Present address: Institute for Integrated Cell-Material Sciences (iCeMS), Kyoto University iCeMS Complex 2, Yoshida Honmachi, Sakyo-ku, Kyoto 606-8501, Japan.

▽ Published ahead of print on 11 April 2011.

tion of LEC apoptosis and histoblast proliferation may contribute functionally to the orderly substitution of cell types without changing the area of the epithelium (49). This implies that the status of proliferation or apoptosis is somehow communicated between the LECs and histoblasts. Several hypotheses that could explain the replacement of abdominal epithelium have been proposed, including mutual signaling events, mechanical forces, or cell competition (49). However, it is currently unknown precisely how LEC apoptosis is triggered and executed in the dynamic remodeling process, and there is little evidence about where and how LEC apoptosis and histoblast proliferation are coupled.

Here, to verify the existence of a relationship between LEC apoptosis and histoblast proliferation, we studied the spatiotemporal pattern of LEC apoptosis by live imaging analysis and developed a system to assay the effect of histoblast proliferation on LEC apoptosis in living animals. We previously reported a genetically encoded fluorescence resonance energy transfer (FRET)-based caspase-3 indicator, SCAT3, which enables the quantitative monitoring of caspase-3-like DEVDase activity (25, 30, 31, 33, 34, 63, 64). By monitoring caspase activation during the epithelial replacement *in vivo* at single-cell resolution, we characterized the activation of caspase in LECs and found that it is regulated by the interactions of the LECs with proliferating histoblasts. Finally, by specifically manipulating histoblast proliferation and using the cell cycle monitoring probe S/G2/M-Green, we found that local interactions with histoblasts transitioning from the S/G_2 cell cycle phases are necessary to trigger caspase activation in LECs at the boundary between the cell populations.

MATERIALS AND METHODS

Fly stocks. The following fly strains were used: *UAS-SCAT3* (25), *UAS-SCAT3*(*DEVG*), *UAS-S/G2/M-Green*, *UAS-nls-SCAT3* (31), *UAS-p35* (a gift from B. Hay), *UAS-dap* (37), *UAS-EcR*-RNAi (59), *UAS-PTEN* (15), *UAS-dMyc* (24), *en-Gal4*, *hh-Gal4* (a gift from T. Tabata), *tsh-Gal4* (a gift from S. Nosseli), *esg-Gal4*, *act-Gal4*, *69B-Gal4*, *AyGal4*^{25} (*Act FRT y*$^{+}$ *FRT Gal4*), *tubP-LexA*::*GAD* (36), *lexAop-SCAT3*, *Nrg-EGFP*^{G305} (48), *hh*^{PyR215} (1), *hsp-flp*^{122}, and *His2Av-mRFP* strains. To generate the *esg* and *cdc2* mutants, *esg*^{VS8} (18), *esg*^{G66B} (26), or *Dmcdc2*^{B47}, *Dmcdc2*$^{E1-24}$ (62) were used as allelic combinations in transheterozygotes. *Drosophila* crosses for the inhibition of histoblast proliferation (*Dap* or *EcR*-RNAi expression under the control of *esg-Gal4*) were done at room temperature (20 to 22°C) to avoid early lethality. Other genetic crosses were carried out by standard procedures at 25°C.

Live imaging and FRET imaging. Most of the sampling steps for pupa imaging are described in detail in a previous report (31). Time-lapse images were captured using an inverted Leica microscope (DMI 6000B) with a spinning disc-type confocal unit (CSU10; Yokogawa) or a Leica SP5 confocal microscope at 22°C. Live imaging of caspase activation during dorsal closure in embryo was performed as described in a previous report (63) with modifications. Confocal FRET images were taken with a Leica microscope equipped with CSU10 and CoolSNAP HQ (Roper Scientific), controlled by the MetaMorph software (Molecular Devices). Time-lapse intervals were 3 to 8 min. The changes in FRET ratio were normalized (divided by the initial ratio values) for Fig. 1F and 2C. Caspase-activated LECs were determined with respect to a normalized ratio value of below 0.7, as indicated in Results. The image analysis was performed using MetaMorph software or ImageJ (NIH Image). Photoshop (CS3; Adobe) was used to adjust brightness and contrast. In most cases, the animal survived during the data acquisition and developed into an adult.

Combination of the GAL4/UAS system and the LexA/*lexAop* system. The GAL4/upstream activation sequence (UAS) system was used to overexpress genes specifically in histoblasts. The *esg-Gal4* driver was used as a histoblast driver. The LexA/*lexAop* system was used to monitor caspase activation in LECs. *tubP-LexA*::*GAD* was strongly expressed in LECs in the abdominal epithelium, although the expression of this driver can be ubiquitously detected in many tissues, including weak expression in histoblasts. Since FRET imaging requires strong expression of the probe, we used binary expression systems such as the LexA/*lexAop* system together with the GAL4/UAS system to obtain quantitative live imaging data.

Plasmid construction. For live imaging of cell cycle dynamics (S/G_2/M phases) *in vivo*, the fragment encoding mAG-hGem (1/110), which is a part of human Geminin (amino acids 1 to 110) with monomeric Azami Green, from pcDNA3 (57) was inserted into pUAST (pUAST-S/G2/M-Green).

To monitor caspase activation using the LexA/*lexAop* system, we constructed a vector containing *SCAT3* under control of the *lexA* operator (*lexAop*) sequence. We constructed a plexAop vector as follows. We amplified the *lexAop* sequence from the yeast two-hybrid vector pSH18-34 with primers 5′-ACGGATCCAAT CTTACCTCG and 5′-ACGGATCCGCATTATCATCC. Partially digested pUAST (BamHI) was prepared to insert the fragment of the PCR product (5′-ACGGATCCGAGCGGAGACTC and 5′-AGGAATTCCCAATTCCCTA TTC) containing pUAST's *hsp70* TATA box and multiple cloning sites with BamHI and EcoRI (the resulting plasmid is pUAST without the UAS). The *lexAop* sequence was then inserted into the BamHI-digested pUAST without the UAS to create the plexAop vector. This vector was structurally similar to pLOT (36). plexAop-SCAT3 was constructed by subcloning the BamHI-HindIII fragment of *SCAT3* from pcDNA3-SCAT3 (64) into the BglII-NotI site of the plexAop vector. Using this construct, *lexAop-SCAT3* transgenic flies were generated.

Manipulation of histoblast proliferation with a near-UVA laser. Histoblast proliferation was inhibited using a near-UVA diode laser (405 nm), and the timing was chosen by monitoring histoblasts in living pupae under the Leica SP5 microscope. Histoblasts were encircled to define the region of interest (ROI), digital zoom was applied (about an 8- to 15-fold increase), and then a strong laser beam (30 to 80% of maximal output) was used to illuminate the cells for a maximum of ~1 min. The illuminated areas were discernible by the photobleaching of the fluorescent proteins (SCAT3 or S/G2/M-Green). The UV treatment was repeated 2 or 3 times (without overlapping) until the fluorescent proteins of histoblasts in the ROI were almost entirely photobleached. UV irradiation may induce an unhealthy status of histoblasts. It is possible that endogenous cell death could eventually be enhanced after UV laser exposure. However, we focused on the initial stage of the replacement (16 to 24 h APF) in our UV laser experiments and following measurements. During this time course, we observed an amount of histoblast apoptosis similar to that as seen under wild-type conditions (4), and most of the UV-treated histoblasts start to proliferate at 10 h after irradiation (see Fig. 5B).

To calculate the histoblast nest expansion, we measured the area of the anterior dorsal histoblast (ADH) at 18 and 24 h APF from the time-lapse imaging data and normalized their values (see Fig. 6B). Histoblasts were arrested in S/G_2 phases, because a longer duration of S/G2/M-Green accumulation in the nuclei was observed after the UV exposure (see Fig. 5A and B).

For the other control experiment, we illuminated only the boundary LECs under the same conditions, but we observed no effects on LEC apoptosis or the replacement process itself.

Analysis with histoblast overexpression clones. To clonally overexpress cell proliferation regulators in histoblasts, we used the FLP-out clone system by generating the line *hs-flp*^{122}; *Act FRT y*$^{+}$ *FRT Gal4 UAS-SCAT3/CyO*. To generate clones of histoblasts, we heat shocked third-instar larvae for 30 min to 1 h at 37°C. After the heat shock, flies were raised at 29°C until the observation period.

Immunohistochemistry. The primary antibodies used were mouse anti-cyclin E (1:10; a gift of H. Richardson), rabbit anti-PH3 (1:500; Upstate Technologies), and rat anti-green fluorescent protein (anti-GFP) (1:250; Nacalai Tesque Inc.). Secondary antibodies were anti-rabbit IgG–Cy5 (1:250; Jackson ImmunoResearch Laboratories, Inc.), anti-mouse IgG–Cy3 (1:250; Jackson ImmunoResearch Laboratories, Inc.), and anti-rat IgG–Alexa Fluor 488 (1:250; Invitrogen).

Immunohistochemistry was performed according to the following procedure (J. H. Yoder, unpublished protocol). Staged pupae were dissected bilaterally with a scalpel with a number 11 blade. The abdominal epidermis was kept attached to the pupal case until mounting. To remove internal organs, the dissected samples were cleaned by gently pumping 1× phosphate-buffered saline (PBS) into the abdomen. Fixation was performed for 1 h at room temperature in 4% paraformaldehyde. The samples were washed three times with 1× PBS and then blocked for 1 h in PBS supplemented with 5% bovine serum albumin (BSA). They were then incubated with the primary antibodies overnight at 4°C in 1× PBS (with no rocking). The samples were washed three times with 1× PBS, blocked again at room temperature in PBS supplemented with 5% BSA, and then incubated with secondary antibodies for 3 h at room temperature in 1× PBS. The secondary antibodies were removed, and the samples were washed with 0.1% Triton X-100–PBS (PBST) and then with 1× PBS three times. To mark the

nuclei, the epidermis was incubated with Hoechst 33342 (2 μM) for 10 min. Finally, the tissue was washed twice with 1× PBS and equilibrated in Slowfade Gold (Invitrogen). The pupal epithelium was pulled from the case with forceps and mounted.

RESULTS

***In vivo* system for the monitoring caspase activation at the single-cell level.** SCAT3 permits *in vitro* monitoring of caspase activation before apoptotic morphological changes, such as nuclear fragmentation (64). To reveal the spatiotemporal patterns of apoptosis during abdominal epithelial replacement *in vivo*, we used flies that express SCAT3 (SCAT3 flies) under control of a *tsh-Gal4* driver, which is expressed in the abdominal epithelium of pupae and is especially strong in LECs (Fig. 1A and B). We first examined the caspase activation dynamics of individual LECs quantitatively *in vivo* by measuring the caspase activation kinetics (i.e., the temporal profiles of the FRET ratio value). A ubiquitous nuclear marker (His2Av-mRFP) was expressed in combination with SCAT3 to facilitate the tracking of caspase activation at the single-cell level. LECs that exhibited caspase activation in the time-lapse data adopted apoptotic morphologies and were gradually removed from the epithelium (Fig. 1C to E; see Movie S1 in the supplemental material). The temporal profiles of FRET ratios in LECs showed that the apoptotic morphological changes and cell extrusion from the epithelium occurred after a severe reduction of FRET (Fig. 1F and G).

To further confirm that the FRET reduction in dying LECs in SCAT3 flies was induced by caspase activation, we prepared transgenic flies expressing SCAT3(DEVG), which contains a sequence that is not cleavable by caspase-3 (Fig. 1H), or we coexpressed SCAT3 and the caspase inhibitor p35 (Fig. 1I). Because neither of these conditions elicited a FRET reduction, the observed FRET reduction in SCAT3 flies reflected caspase activation. Therefore, this system allows us to confirm for the first time the location of individual cells exhibiting caspase activation and to quantitatively evaluate caspase activation dynamics at the single-cell level during tissue remodeling in living animals.

Caspase activation in LECs is induced mainly at the boundary with histoblasts during epithelial replacement. Live imaging analysis of SCAT3 flies revealed that all the LEC removal in normal development is mediated by caspase activation. We analyzed the spatiotemporal pattern of caspase activation in detail, focusing on the spatial pattern of the caspase activation in LECs. To quantify these observations, we categorized the LECs starting to show caspase activation. In our measurements, the caspase-activating LECs apposed to histoblasts at the LEC/histoblast boundary were classified as "boundary" LECs, and those LECs that did not contact histoblasts were classified as "nonboundary" LECs (Fig. 2A). For these analyses, we defined the caspase-activated state as the ratio below a threshold that had a normalized value of 0.7 (see Materials and Methods). We chose this value because in most apoptotic LECs, once this value was exceeded, the maximum activation (i.e., minimum FRET value) or apoptosis (confirmed by apoptotic cell fragmentation) was observed within 1 h.

Caspase activation was frequently observed in the boundary LECs, which were in close contact with histoblasts (see Movie S1 in the supplemental material). The quantification of the distribution of caspase-activated LECs indicated that approximately 85% were at the boundary during epithelial replacement (18 to 30 h APF) (Fig. 2B, panel b). A time course analysis at 2-hour intervals showed a similar distribution of caspase-activated LECs (Fig. 2B, panel a), suggesting that most LEC apoptotic events were induced at the LEC/histoblast boundary, which progressed as the LECs were eliminated.

To confirm whether the interaction between histoblasts and LECs correlated with the initiation of caspase activation, we also measured the time between a histoblast being apposed to an individual LEC and caspase activation in that LEC. We found that direct apposition between individual LECs and histoblasts almost always preceded caspase activation in the LECs (Fig. 2C). Although there was cell-to-cell variability in the time required for the FRET ratio to pass the threshold after the apposition (169 ± 115 min; $n = 65$ boundary LECs), a sharp FRET ratio reduction below the threshold to apoptosis in LECs was observed after the threshold was exceeded (26.0 ± 17.7 min). The histoblast-LEC proximity is therefore probably related to the initiation of caspase activation in boundary LECs. In contrast, nonboundary LECs usually showed temporal profiles of FRET ratio changes similar to those for boundary LECs, but some of them did not show a sharp gradient of temporal profiles. In this case, caspase activation frequently seemed to last for a long time without reaching maximum activation and without apoptosis (see Movie S1 in the supplemental material), indicating an irregular caspase activation pattern. Since such irregular caspase activation was not observed in the boundary LECs, the boundary regulation of caspase activation could function to induce apoptosis at a constant frequency during the replacement process.

To test the general hypothesis that caspase activation occurs at the boundary of different cell populations, we focused on dorsal closure (DC) in *Drosophila* embryogenesis. During DC, the amnioserosa (AS) cells and the lateral epidermis, especially the leading edge (LE), are the two populations that form a boundary. Previous reports showed that about 10% of AS cells undergo apoptosis and suggested that this contributes to the physical forces required for the closing process (27, 65). In case of the AS/LE interaction, unlike the histoblast/LEC interaction, both cell populations are nonproliferative. We examined the spatiotemporal pattern of caspase activation in AS cells during DC and found that AS apoptosis seemed to occur randomly (Fig. 2D and E) rather than at the AS/LE boundary (Fig. 2B, panel b). Taken together, these results suggest that the regulation of apoptosis at the boundary between tissues may be a specific characteristic of abdominal epithelial replacement.

Histoblast nest expansion, which is mediated by proliferation, regulates the frequency of caspase activation in neighboring LECs. To investigate how caspase activation in LECs is regulated, we focused on the interactions between the two cell types. The idea that LEC death is nonautonomous was originally suggested as speculation more than 30 years ago in a study that ablated histoblasts (55). The proliferation of histoblasts has been reported to be required for the efficient removal of LECs (49). We examined flies with mutations in *escargot* (*esg*) or *Dmcdc2* (*cdc2*), whose products are necessary to maintain the diploidy of histoblasts (17, 18). These mutant

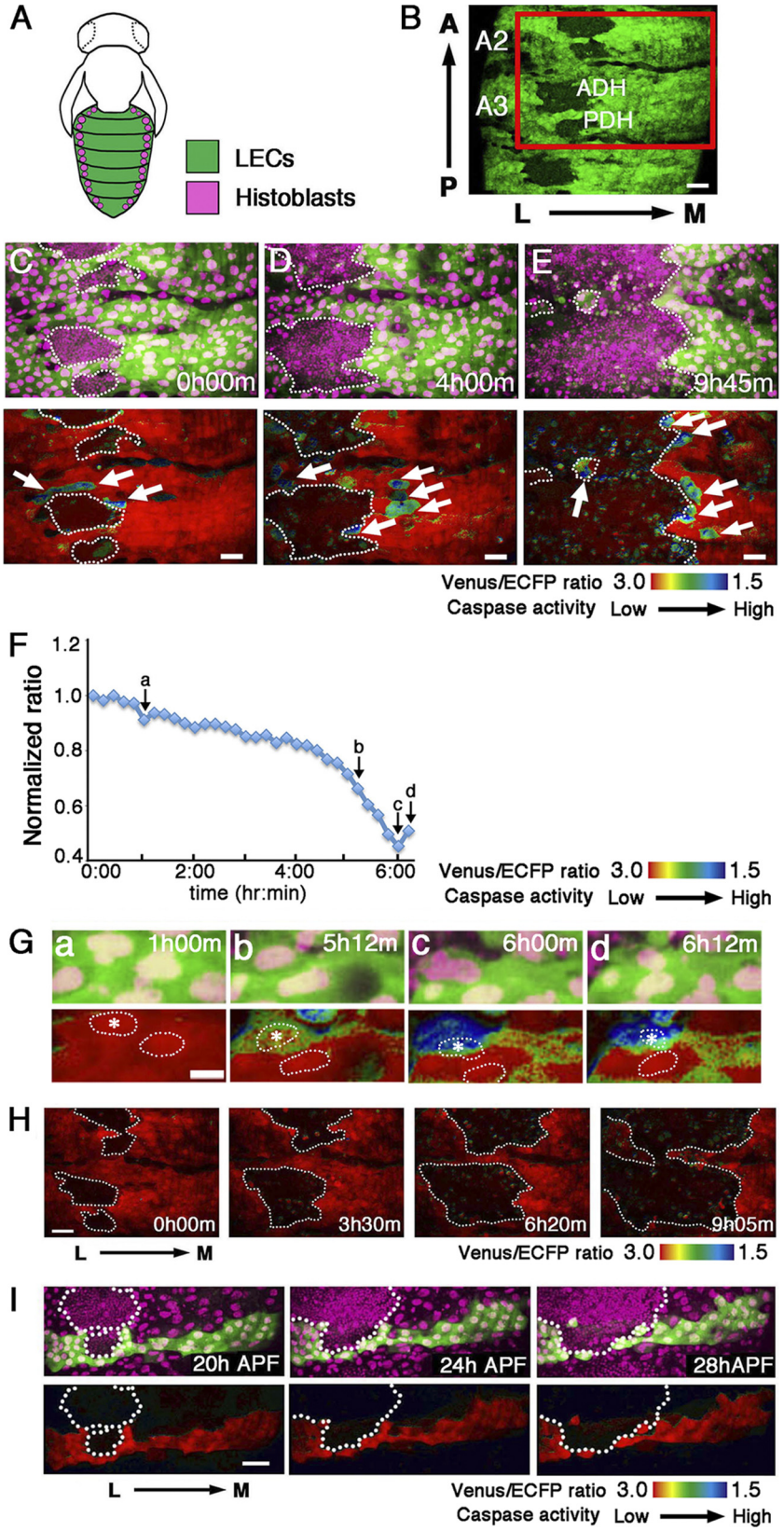

FIG. 1. Single-cell level caspase activation dynamics in LECs during epithelial replacement. (A) Schematic illustration of the dorsal abdominal epidermis of a pupa. (B) Expression pattern of an epithelial driver, *tsh-Gal4*, in the pupal abdomen (A, anterior; P, posterior; L, lateral; M, medial). In each dorsal segment, there are anterior dorsal histoblast (ADH) nests and posterior dorsal histoblast (PDH) nests. The boxed area (segments A2 and A3) was monitored. The expression of fluorescent proteins (SCAT3) in histoblasts is not clear because the expression was low. (C to G)

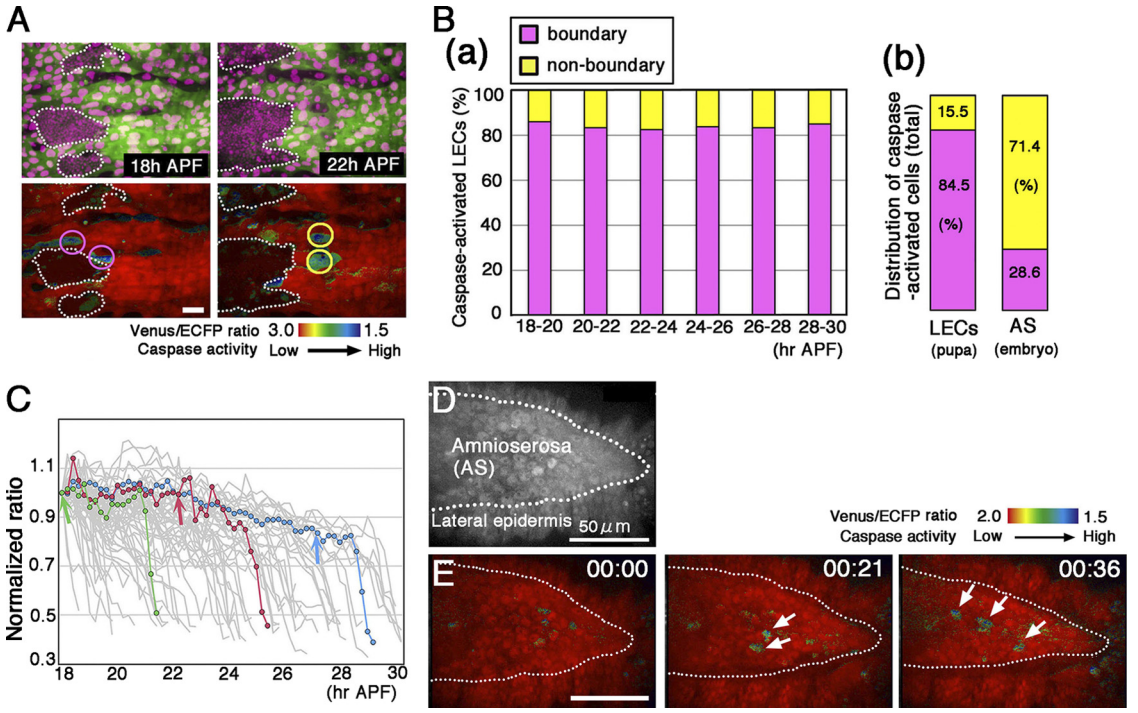

FIG. 2. Initiation of caspase activation in LECs starts mainly at the boundary between LECs and histoblasts. (A) Categories for showing the location of caspase-activated LECs. Magenta circles show caspase-activated LECs at the "boundary," and yellow circles show the "nonboundary" caspase-activated LECs. Scale bar, 50 μm. (B) Panel a, distribution of caspase-activated LECs at 2-hour intervals, categorized as in panel A (n = 214 LECs; 3 segments). Panel b, distribution of caspase-activated cells in the larval epidermis during abdominal replacement in the pupa (left) and in the AS during DC in the embryo (right) (n = 42 cells; 3 flies). (C) Kinetics of the FRET ratio of individual caspase-activated boundary LECs. Data for 65 individual LECs are shown (gray lines). Three representative LECs exhibiting caspase activation at early, intermediate, or late replacement times are highlighted in green, red, and blue, respectively. The arrows indicate the time of histoblast apposition for each highlighted LEC. The genotype was *tsh-Gal4 UAS-SCAT3/His2Av-mRFP.* (D and E) SCAT3 is expressed in the epidermis of an embryo. CFP (D) and FRET ratio (E) images of a SCAT3-expressing embryo are shown. Snapshots show the spatiotemporal pattern of caspase activation in AS cells during DC. The dashed line shows the boundary between AS cells and the LE cells of the lateral epidermis. The elapsed time (min) is shown. The arrows show AS cells with activated caspase. The genotype was *UAS-SCAT3*/+; *69B-Gal4*/+. Scale bars, 50 μm.

flies showed severe abdominal defects, because their histoblasts become polyploid, entered the endoreplication cycle, and failed to proliferate normally during metamorphosis. In both mutants, the histoblast nests remained in their lateral positions, and significant defects in LEC elimination were observed (Fig. 3A to C).

To evaluate whether the initiation of caspase activation in the LECs adjacent to histoblasts is correlated with histoblast proliferation, we blocked their proliferation and monitored the spatiotemporal caspase activity in LECs by live imaging. To assay this effect, we developed a method that combined the GAL4/UAS system and the LexA/*lexAop* system (36). This allowed us to overexpress genes specifically in histoblasts and observe caspase activation in the LECs quantitatively *in vivo*. Ninov et al. showed that interference with reception of the Ecdysone signal (overexpression of *EcR*-RNAi) or overexpression of the cyclin-dependent kinase inhibitor Dacapo (*Dap*) (37) in histoblasts strongly inhibited their proliferation (49). We first quantified the effect on caspase activation in LECs at the boundary and counted the number of caspase-activated LECs (16 to 24 h APF) (Fig. 3D to F). During this time course, the nest size of the histoblasts expressing either Dap or EcR-RNAi did not change much (Fig. 3G), indicating that few histoblasts had divided. In the control flies, almost all of the

Measurement of FRET ratio changes at the single-cell level. Nuclei are marked by ubiquitously expressed His2Av-mRFP (magenta), and the abdominal epidermis is labeled by SCAT3 (Venus image) (green). SCAT3 ratio images are shown in the lower panels. Arrows indicate caspase-activated LECs. Time-lapse imaging was begun at 18 h APF. The elapsed time is shown. The dashed lines indicate the boundary between the histoblasts and LECs. (F) Typical kinetics of the FRET ratio of an LEC. (G) Ratio images and corresponding morphological changes. Two representative nuclei are outlined by a dashed line. The kinetics of the FRET ratio of a single LEC (*) is drawn in panel F, and the arrows labeled a to d in panel F correspond to panels a to d in panel G. The genotype of the SCAT3 flies was *tsh-Gal4 UAS-SCAT3/His2Av-mRFP.* (H and I) Confirmation of FRET reduction for SCAT3 imaging. (H) FRET ratio images of the caspase noncleavable SCAT3, SCAT3(DEVG). The fly genotype was *tsh-Gal4 UAS-SCAT3*(*DEVG*)/*CyO.* The time-lapse imaging was begun at 18 h APF. The elapsed time is shown in each panel. (I) FRET ratio images from a fly expressing *p35* in the posterior compartment. The genotype was *en-Gal4 UAS-SCAT3/His2Av-mRFP*; *UAS-p35*/+. The dashed line shows the boundary of histoblast nests. L, lateral; M, medial. Scale bars, 50 μm (B, C, D, E, H, and I) and 20 μm (G).

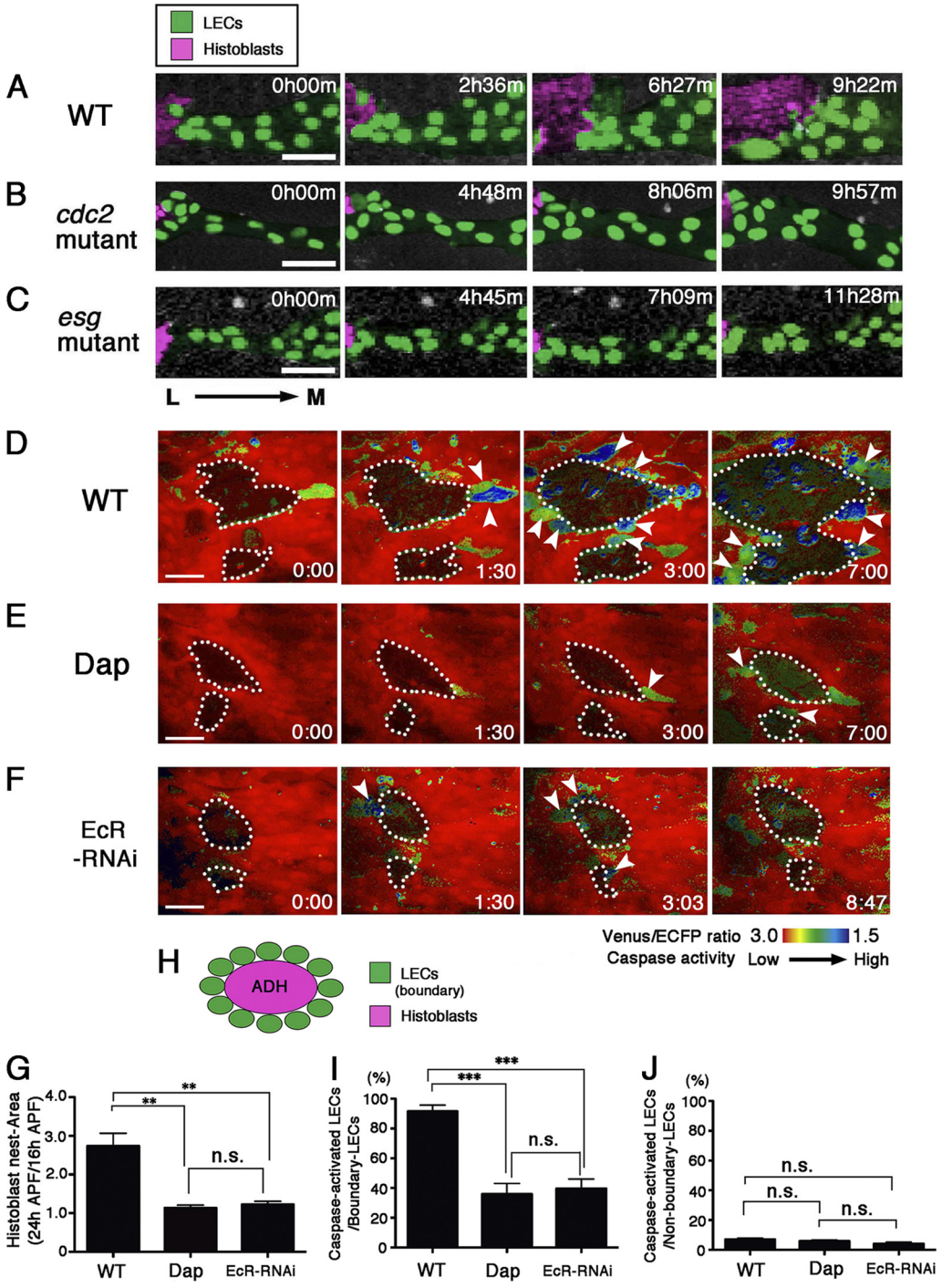

FIG. 3. Histoblast nest expansion regulates the frequency of caspase activation in the "boundary" LECs. (A to C) Defective LEC death in histoblast proliferation mutants. Time-lapse imaging was performed from 18 h APF. The elapsed time is shown for each panel. Histoblasts and LECs are shown in magenta and green pseudocolor, respectively. The genotypes were as follows: (A) Wild type (WT) (*hh-Gal4 UAS-nls-SCAT3*/+); (B) *cdc2* mutant ($Dmcdc2^{E1\text{-}24}$/$Dmcdc2^{B47}$; *hh-Gal4 UAS-nls-SCAT3*/+); (C) *esg* mutant (esg^{VS8}/esg^{G66B}; *hh-Gal4 UAS-nls-SCAT3*/+). L, lateral; M, medial. (D to F) Monitoring system for the effects of genetically modified histoblasts on caspase activation in LECs. SCAT3 is expressed by the LexA/*lexAop* system, and the GAL4/UAS system is used for histoblast-specific expression. The elapsed time (h:min) is shown for each panel. (E and F) *UAS-dacapo* (*dap*) or *EcR* (*Ecdysone Receptor*)-RNAi constructs were overexpressed by the *esg-Gal4* driver. Arrows indicate caspase-activated LECs at the boundary between the LECs and histoblasts. (G to J) Anterior regions and ADH nests are the focus of the following results. (G) Expansion of the histoblast nest over the 8-h interval between 16 h and 24 h APF. Histoblast nest expansion was severely impaired when histoblast proliferation was inhibited. (H) LECs located adjacent to the ADH in the A3 segment at the initial stage (16 h APF, ellipses) were analyzed. (I) Frequency of caspase activation in the boundary LECs. The ratio of the caspase-activated LECs at the boundary to the total boundary LECs is shown (WT, $n = 5$ flies; Dap, $n = 4$ flies; EcR-RNAi, $n = 4$ flies). (J) Frequency of caspase activation in nonboundary LECs. The ratio of nonboundary caspase-activated LECs to the total LECs in the vicinity of wild-type or proliferation-defective histoblasts is shown (WT, $n = 4$ flies; Dap, $n = 4$ flies; EcR-RNAi, $n = 4$ flies). Fifty to 75 LECs in the anterior region were counted for each individual. (G, I, and J) One-way analysis of variance (ANOVA) with Tukey-Kramer test: ***, $P < 0.0001$; **, $P < 0.01$; n.s., not significant). Genotypes: WT, *tubP-LexA*::*GAD*; *esg-Gal4 lexAop-SCAT3*/*CyO*; Dap, *tubP-LexA*::*GAD*/+; *esg-Gal4 lexAop-SCAT3*/*UAS-dap*; EcR-RNAi, *tubP-LexA*::*GAD*/+; *esg-Gal4 lexAop-SCAT3*/+; *UAS-EcR*-RNAi/+. Scale bars in panels A to F, 50 μm.

LECs at the boundary exhibited caspase activation during the observation period (Fig. 3D and I). In contrast, in the flies in which histoblast proliferation was inhibited, the number of caspase-activated LECs at the boundary was significantly lower (Fig. 3E, F, and I). To determine whether the caspase activation affected by proliferating histoblasts is limited to boundary LECs, we quantified the frequency of caspase activation in nonboundary LECs under the experimental conditions described above. Intriguingly, the rates of caspase activation in the nonboundary LECs did not differ significantly in the control and proliferation-defective histoblast lines (Fig. 3J). These results together suggested that the inhibition of histoblast proliferation, which causes defects in histoblast expansion, affects the frequency of caspase activation in the neighboring, boundary LECs, resulting in severely delayed LEC removal.

Region-specific manipulation of histoblast proliferation with a UV laser. The experiments described above confirmed that when histoblast proliferation was inhibited in an entire histoblast nest, the autonomous effect was the impairment of histoblast nest expansion, which resulted in simultaneous migration defects. From these data, it was not clear whether histoblast expansion as a whole, supposedly producing mechanical forces, or local interactions with proliferating histoblasts were necessary for the apoptosis of the neighboring LECs. To evaluate the more local effects of cellular interactions on LEC apoptosis, we tried manipulating histoblast proliferation in restricted subsets of histoblasts *in vivo*.

The exposure of proliferating mammalian cells to UVA (320 to 400 nm) causes the production of reactive oxygen species (ROS) or impaired proteasomal function, which inhibits cell cycle progression at the G_2/M phase (7, 16). We carefully exposed histoblasts to near-UVA diode laser illumination (405 nm) under the confocal microscope to find a level that would inhibit their proliferation without killing them (see Materials and Methods). We verified the viability of the histoblasts by monitoring their recovery of fluorescence over time. In most cases, the illuminated histoblasts regained fluorescent protein expression and remained in the epithelium for the time of our observation (~12 h) without specific signs of cellular damage, but they did not divide for approximately 10 to 12 h. When the histoblasts were exposed to an optimized dose of UV laser illumination, the expansion of the histoblast nest was severely impaired (see Fig. 6A and B), just as for the histoblasts whose proliferation was genetically inhibited (Fig. 3G). This setup allowed the region-specific manipulation of histoblast proliferation and direct examination of the involvement of proliferating histoblasts with LEC apoptosis.

Cell cycle progression of histoblasts is necessary to induce nonautonomous apoptosis in neighboring LECs. To examine whether cell cycle arrest actually occurs in histoblasts after UV laser exposure, especially at specific phases, we first characterized the cell cycle dynamics of histoblasts during abdominal epithelial replacement. Sakaue-Sawano et al. previously reported the development of an indicator molecule for cell cycle progression (57). We used this construct (called S/G2/M-Green), which permits cells in the S/G_2 and M phases to be detected and monitored over time, (Fig. 4A), to generate transgenic flies. In the S/G2/M-Green transgenic flies, the probe accumulated in the nuclei of histoblasts in L3 larvae, before the first mitosis of pupariation, indicating that the cells were in S/G_2 phase (Fig. 4B and C). At 2 h APF, histoblasts divide almost in synchrony, which was confirmed in our system by the distribution of S/G2/M-Green from the nucleus to the cytoplasm, which signals entry into the M phase (Fig. 4D). These observations are consistent with previous reports indicating that histoblasts are arrested in the G_2 phase until after the beginning of pupariation (35, 50). Since histoblasts pass through the conventional cell cycle phases (G_1/S/G_2/M) during pupariation, nuclear accumulation of the probe probably reflects their S/G_2 phases (Fig. 4E to G; see Movie S2 in the supplemental material). Moreover, we examined the accumulation of cyclin E, a marker for the late G_1 phase (28), in the pupa at the replacement stage by immunohistochemistry. We found that cyclin E was concentrated in histoblasts that were not in the S/G_2 phase, as judged by S/G2/M-Green accumulation in the nucleus (Fig. 4H and Table 1). We also detected the M phase by anti-phospho-histone H3 (PH3) staining and confirmed that the PH3-positive cells corresponded to cells with a cytoplasmic distribution of S/G2/M-Green (Fig. 4I and Table 1). These observations suggest that the reporter S/G2/M-Green exclusively reflects the S/G_2 and M phases. Therefore, this probe allowed us to monitor the dynamics of cell cycling through the S/G_2 and M phases at the single-cell level in pupal abdominal histoblasts.

Next, we tried manipulating the cell cycle of histoblasts by our UV manipulation method. After the exposure to UV laser illumination, S/G2/M-Green accumulated at high levels in the nuclei of histoblasts, and their S/G_2 phases lasted much longer than normal (Fig. 5A and B). Under this condition, we investigated the behaviors of LECs in contact with histoblasts which are arrested in S/G_2 phases. We found that the boundary LECs that interacted with histoblasts in the S/G_2 phases did not undergo apoptosis and stayed in the epithelium (Fig. 5D; see Movie S4 in the supplemental material [for a control, see Fig. 5C and see Movie S3 in the supplemental material]). Considering that at the onset of the replacement most of the histoblasts in the nest also stayed in the S/G_2 phases (Fig. 4G), the transition from the S/G_2 phases might set in motion the cellular mechanism that triggers the apoptosis in the boundary LECs.

Since S/G2/M-Green enables us to monitor the cell cycle progression of pupal histoblasts in living flies, we focused on the cell cycle phases of the histoblasts surrounding dying LECs (confirmed by their apical constriction and extrusion from the epithelium). We took data for about 10 to 12 h from 16 h APF, and at least during this period, the length of S/G_2 phase did not seem to change. During the replacement, about two-thirds of all the histoblasts were in the S/G_2 phases (Fig. 4F), indicating that about one-third were in the M or G_1 phase. Intriguingly, during LEC apoptosis, more than 50% of the adjacent histoblasts transited from the S/G_2 phase (ration, 0.53 ± 0.27 [mean ± standard deviation]) (n = 77 LECs), suggesting that histoblasts shifted from the S/G_2 phase to M or G_1 at a high frequency at the boundary (Fig. 5C; see Movie S3 in the supplemental material). We examined the duration of the S/G_2 phases of histoblasts and found that the histoblasts at the boundary showed a shorter period of S/G_2 phases (185.3 ± 50.4 min), compared to the average length of S/G_2 phases (217.8 ± 64.3 min). This result could also support the high frequency of the cell cycle phase shift of the adjacent histo-

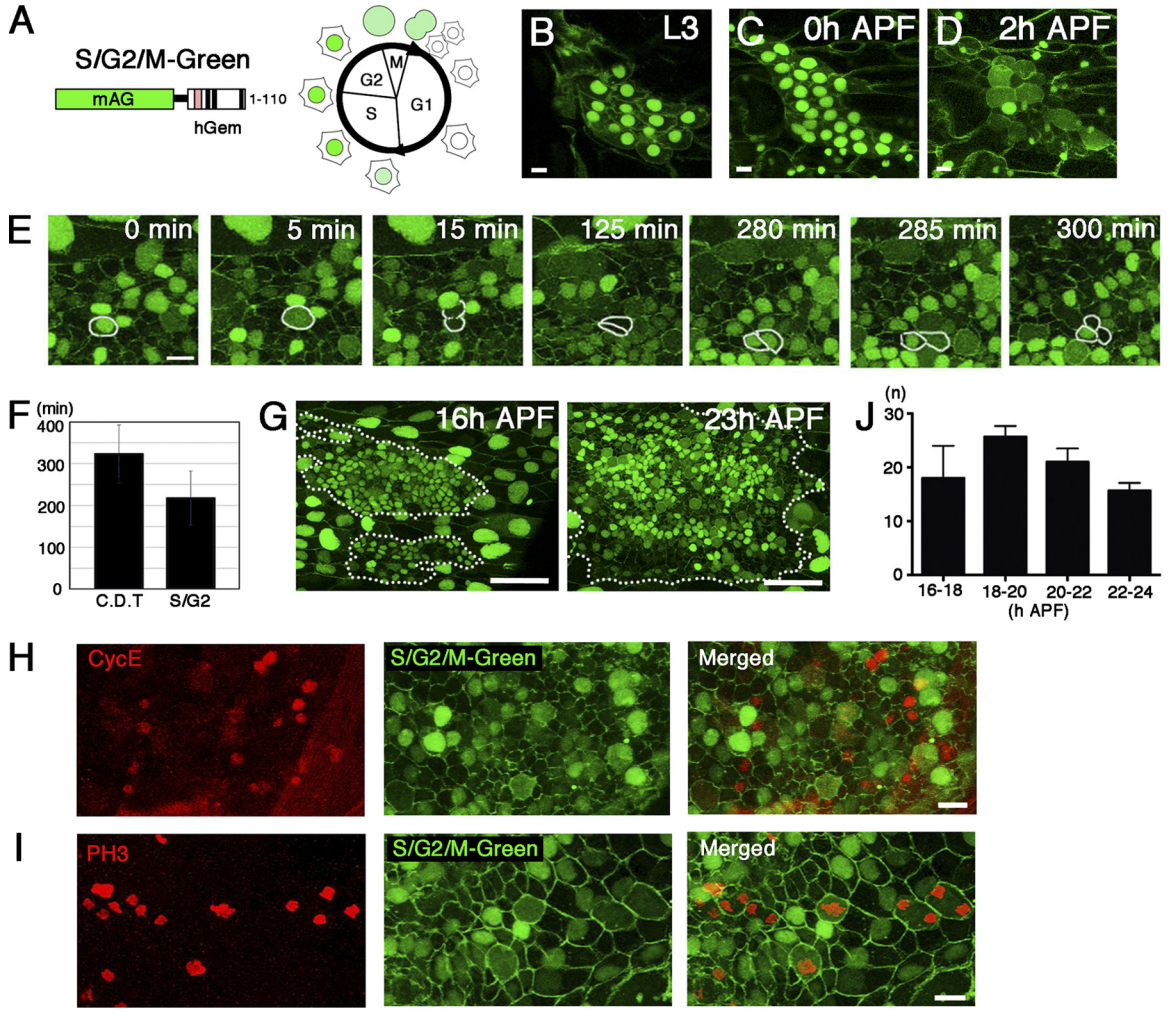

FIG. 4. Cell cycle dynamics of histoblasts monitored by S/G2/M-Green. (A) S/G2/M-Green, a fluorescent probe that labels cells in the S/G_2/M phases. In the construct, mAG (monomeric Azami Green) is fused to the deletion mutant of human Geminin (57). Accumulation of S/G2/M-Green in the nucleus indicates that the cell is in the S/G_2 phase. Distribution of S/G2/M-Green into the cytoplasm corresponds to the initiation of M phase. (B and C) S/G2/M-Green accumulated in histoblasts in the L3 larval stage and before the first mitosis upon pupation (0 h APF). (D) Histoblasts undergo synchronous division at around 2 h APF. (E) Time-lapse observation of cell cycle changes of histoblasts during the replacement stage (from 15 h APF). Cellular outlines are marked by Nrg-GFP. White lines indicate the example. (F) Average cell doubling time (C.D.T) and duration of the S/G_2 phases of the histoblasts (C.D.T., $n = 47$; S/G_2 phase, $n = 127$). S/G_2 phase was monitored by examining S/G2/M-Green flies, and C.D.T. was also counted by time-lapse analysis using His2Av-RFP lines (from 16 h APF). (G) Left, at the initial stage of replacement, most histoblasts were in the S/G_2 phase. Right, cell cycle progression occurs dynamically in histoblasts throughout the expanding nest. The white dashed lines indicate histoblast nests. (H and I) S/G2/M-Green indicates the S/G_2 and M phases but not the G_1 phase. (H) Cyclin E accumulated in histoblasts that did not show an accumulation of S/G2/M-Green in the nucleus. (I) M phase cells were recognized by their round or dividing shape using a cell shape marker (Nrg-GFP). These cells showed a cytoplasmic distribution of S/G2/M-Green and coincided with PH3-positive cells. (J) Frequency of G_2/M transition in histoblasts surrounding LECs. The number of histoblasts passing from G_2 to M phase surrounding LECs was counted in 2-h intervals. Three individual flies were tested. The frequency of the G_2/M transition of histoblasts was not different significantly between time courses (one-way ANOVA with Tukey-Kramer test). Cells with large nuclei are LECs in panels E and G. The genotype of S/G2/M-Green flies was *Nrg-GFP*; *act-Gal4 UAS-S/G2/M-Green/CyO*. Scale bars, 10 μm (B to E, H, and I) and 50 μm (G).

TABLE 1. Distribution of cyclin E-accumulating and PH3-positive cells, corresponding to the dynamics of the S/G2/M-Green signal[a]

Cell cycle phase (S/G2/M-Green)	% (no.) of cells:	
	Accumulating cyclin E ($n = 157$)	PH3 positive ($n = 203$)
S/G_2	3.2 (5)	1.0 (2)
M	1.3 (2)	91.6 (186)
G_1 (not S/G_2)	95.5 (150)	3.9 (8)
Unidentified	0 (0)	3.4 (7)

[a] The cell cycle phases indicated by S/G2/M-Green, anti-cyclin E in the nucleus, and anti-PH3 are shown.

blasts during LEC apoptosis. Furthermore we investigated the frequency of histoblasts transitioning from S/G_2 to M phase surrounding LECs over time and found that the frequency of histoblasts showing G_2/M phase transition did not change significantly between the early and middle stages of the replacement (Fig. 4J), implying that histoblasts constantly show cell cycle progression during the normal replacement. Together with the finding that arresting the cell cycle at the S/G_2 phases inhibited LEC apoptosis (Fig. 5D), these results suggest that the cell cycle progression of histoblasts passing through S/G_2

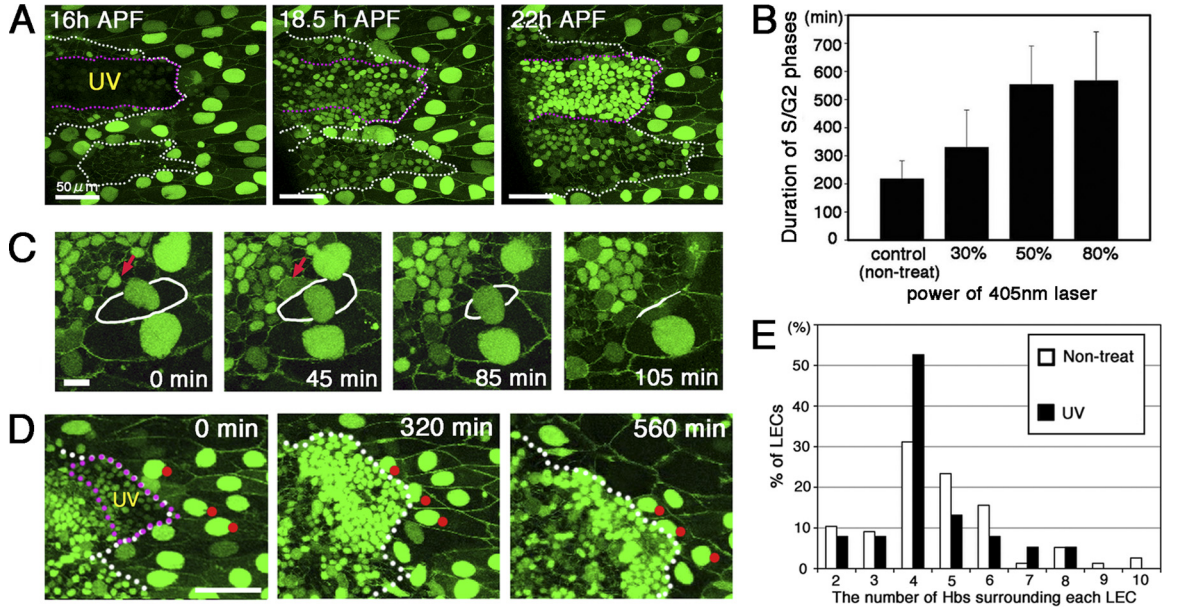

FIG. 5. Normal cell cycle progression of histoblasts is necessary to induce nonautonomous apoptosis in neighboring LECs. (A and B) After UV exposure, S/G2/M-Green accumulated in the nuclei of histoblasts for a much longer time than in the nontreated control. (A) *In vivo* monitoring of S/G2/M-Green accumulation after UV laser illumination. (B) Duration of S/G_2 phases of histoblasts. Each bar shows the time required for histoblasts to pass through S/G_2 phases under several conditions according to the laser (405-nm) power (control, $n = 127$; 30%, $n = 64$; 50%, $n = 27$; 80%, $n = 49$). (C) Stills from a time-lapse movie showing that the cell cycle progression of histoblasts occurs during neighboring LEC apoptosis. LEC apoptosis is defined as delamination from the epithelium (coincident with nuclear fragmentation). The arrow indicates a dividing histoblast. The white line indicates the shape of a dying LEC. (D) Stills from a time-lapse movie showing defects in the apoptosis of LECs neighboring S/G_2 phase-arrested histoblasts. LECs in contact with S/G_2 phase-arrested histoblasts (red dots) did not show delamination during the observation. The white dashed lines indicate histoblast nests. Magenta dashed lines indicate the UV-illuminated region. (E) The number of histoblasts surrounding apoptotic LECs was similar to the number of S/G_2 phase-arrested histoblasts surrounding LECs after UV laser exposure. The graph shows the distribution of the number of histoblasts surrounding each LEC for the following conditions. The number of normal, untreated histoblasts surrounding each LEC during apoptosis was 4.71 ± 1.76 (histoblasts per LEC; $n = 77$ LECs). The number of UV-illuminated histoblasts surrounding individual boundary LECs was 4.42 ± 1.42 (histoblasts per LEC; $n = 38$ LECs). The genotype of S/G2/M-Green flies was *Nrg-GFP*; *act-Gal4 UAS-S/G2/M-Green/CyO*. Scale bars, 50 μm (A and D) and 10 μm (C).

phases is important for coordinating the neighboring LEC apoptosis.

Local interactions with proliferating histoblasts are necessary for caspase activation in boundary LECs. To evaluate quantitatively the effect on caspase activation in the LECs neighboring the UV-illuminated, or cell cycle-arrested, histoblasts, we did following experiments using SCAT3 flies. We used a UV laser to illuminate the anterior dorsal histoblast (ADH) nest of the A3 segment at 16 h APF and monitored the caspase activity by live-imaging analysis (Fig. 6A). Focusing on the LECs initially present at the boundary, we counted the number of caspase-activated LECs (18 to 24 h APF). As with the histoblasts whose proliferation was genetically inhibited, the number of caspase-activated LECs at the boundary significantly decreased when the entire ADH nest was treated with UV laser illumination (Fig. 6C, bars a and b).

Next, we treated only the medial tip (about one-third) of the cells with UV laser illumination and found that the number of caspase-activated LECs decreased by approximately 50% (Fig. 6C, bar c). In contrast, UV illumination of the lateral tip of the ADH nest, which is the opposite side of the focusing boundary LECs, did not significantly alter the frequency of caspase-activated LECs (Fig. 6C, bar d). Considering that the histoblast nest underwent similar amounts of expansion following UV illumination of the medial or lateral ADH nest (Fig. 6B, bars c and d), the contributions of histoblast expansion as a whole seem to be similar under these two conditions. However, the frequency of caspase activation in the boundary LECs showed a significant difference between these (Fig. 6C, bars c and d), suggesting that local interactions between the LECs and proliferating histoblasts trigger caspase activation in the boundary LECs.

Because of the possible pleiotropic effects of UV exposure, we also confirmed the relationship between local histoblast cell cycle progression and nonautonomous LEC apoptosis by clonally overexpressing a cell proliferation regulator in contiguous histoblast clones (FLP-out clones). To select the genes for generating overexpression clones, we first did preliminary screening to determine whether candidate genes could inhibit histoblast proliferation in FLP-out clones and affect the epithelial replacement. We tried inhibition or downregulation of the cell cycle (*Dap* and *string*-RNAi), Ecdysone-signaling (*EcR*-RNAi), epidermal growth factor (EGF) signaling (*EGFR-DN* and *EGFR*-RNAi), and cell growth (*PI3K*-RNAi, *PTEN*, and *dMyc*-RNAi). Among these, PTEN overexpression clones successfully suppressed histoblast proliferation and resulted in delay of the epithelial replacement, whereas clonal overexpression of the other constructs was not effective for preventing cell proliferation. It has been reported that in the replacement stage, the cell cycle progression of histoblasts is

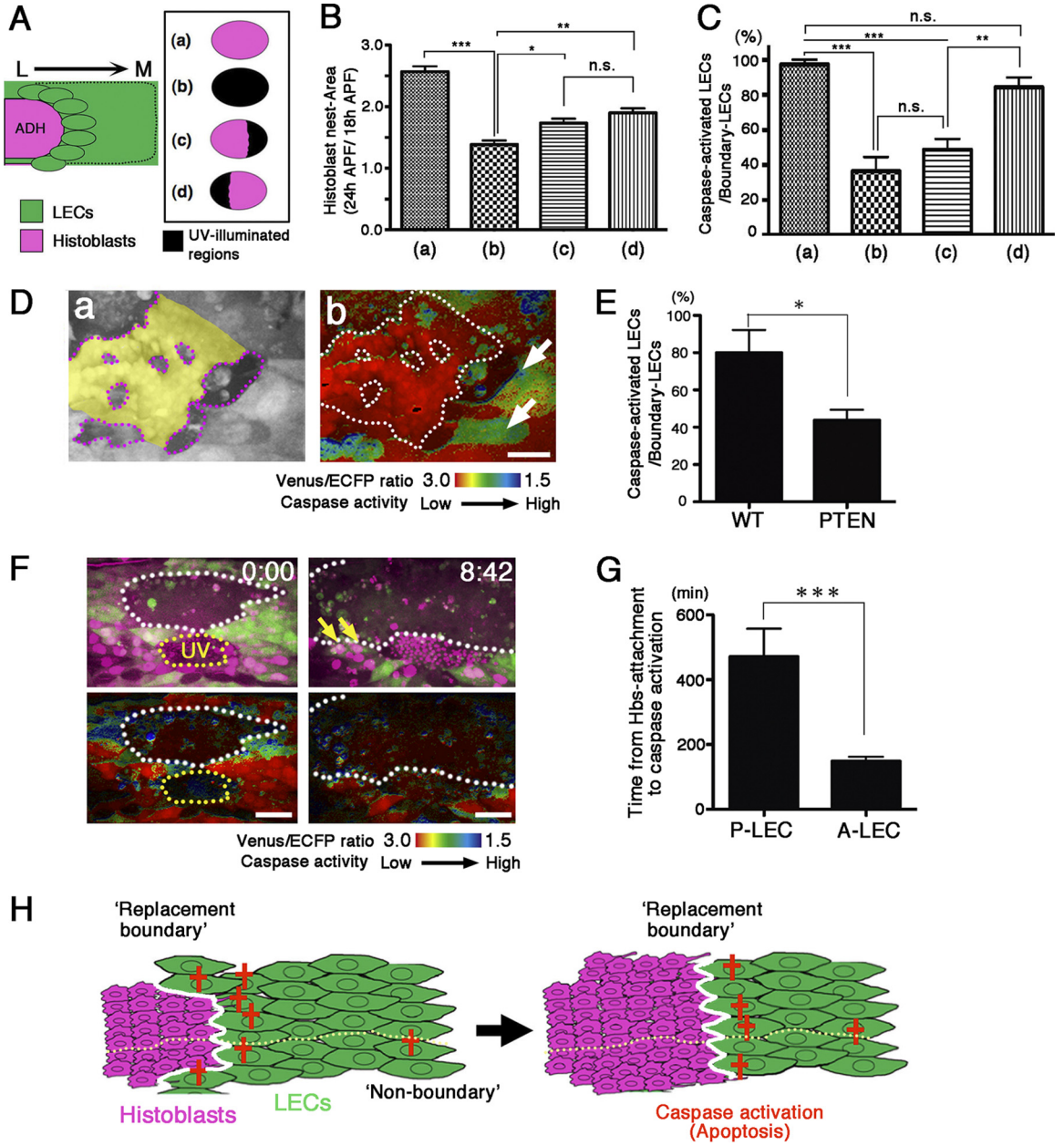

FIG. 6. Local interactions with proliferating histoblasts regulate the frequency of caspase activation in neighboring LECs. (A to C) The frequency of caspase activation in the boundary LECs is regulated by their local interactions with proliferating histoblasts. (A) Medial boundary LECs located adjacent to ADH at the initial stage (ellipses) were analyzed under four UV-illuminated conditions: a, nontreated control; b, entire ADH; c, medial one-third of the ADH; and d, lateral one-third of the ADH. L, lateral; M, medial. (B) Expansion of the histoblast nest (bar a, $n = 4$ flies; bar b, $n = 4$ flies; bar c, $n = 5$ flies; bar d, $n = 6$ flies) (one-way ANOVA with Tukey-Kramer test: ***, $P < 0.0001$; **, $P < 0.01$; *, $P < 0.05$; n.s., not significant). (C) Ratio of the caspase-activated LECs to the total boundary LECs from 18 to 24 h APF (bar a, $n = 5$ flies; bar b, $n = 7$ flies; bar c, $n = 6$ flies; bar d, $n = 8$ flies) (one-way ANOVA with Tukey-Kramer test: ***, $P < 0.0001$; **, $P < 0.01$; n.s., not significant). (D and E) Local interactions with proliferation-defective histoblasts delay caspase activation in neighboring LECs. (D) FLP-Out/FRT UAS-PTEN clones were generated in histoblasts marked with SCAT3. Venus (panel a) and FRET ratio (panel b) images of SCAT3 are shown. The yellow region and white dashed lines indicate PTEN-overexpressing clones in histoblasts; the magenta dashed line indicates neighboring wild-type histoblasts. Arrows indicate caspase-activated LECs in contact with wild-type neighbors. Scale bar, 20 μm. (E) Frequency of caspase activation in boundary LECs interacting with PTEN-overexpressing clones (PTEN) or wild-type neighbors (WT); the ratio of caspase-activated LECs to boundary LECs (WT, $n = 5$ flies; PTEN, $n = 6$ flies) is shown. Observations were made between 16 and 24 h APF. (Unpaired t test, $P = 0.0187$ [<0.05].) (F and G) Local interactions between LECs and histoblasts are restricted by the developmental A/P compartment boundary during epithelial replacement. (F) Snapshots showing an individual with a PDH nest that was entirely UV illuminated. In the upper panels, posterior cell nuclei are marked by an enhancer trap line with nls:DsRed (magenta), and the abdominal epidermis is labeled by SCAT3 (Venus image) (green). Ratio images of SCAT3 are shown in the lower panels. Time-lapse imaging began around 18 h APF. White dashed lines indicate the ADH boundary; yellow arrows indicate posterior LECs in contact with only ADH cells. Elapsed time (h:min) is shown. Scale bars, 50 μm. (G) Duration of anterior or posterior LEC interactions with ADH cells before LEC caspase activation (P LECs, $n = 16$; A LECs, $n = 33$) (unpaired t test: ***, $P < 0.0001$.) (H) Model summarizing the abdominal epithelial replacement. Apoptosis at the "replacement boundary," which moves as the LECs

dependent on cell growth signaling and inhibition of phosphatidylinositol 3-kinase (PI3K) signaling causes cell cycle arrest or very slow histoblast proliferation (50). We inhibited PI3K signaling by overexpressing PTEN in FLP-out clones and found that the frequency of caspase activation in LECs in contact with PTEN-overexpressing histoblasts was lower than in that LECs next to wild-type histoblasts (Fig. 6D and E). This indicates that the local cell cycle progression of histoblasts is necessary for efficient caspase activation in neighboring LECs.

Effects of local interactions between LECs and histoblasts are restricted by the A/P compartment border. Finally, we addressed whether the developmental compartment restricts the effects of local interactions between LECs and histoblasts. In the cell competition between *Minute*/+ and wild-type (+/+) cells, apoptosis occurs progressively in the *Minute*/+ cells at their boundary with wild-type clones (41, 47). However, this boundary effect occurs only between clones in the same developmental compartment (61). In contrast to the static growth of the imaginal discs, where this cell competition takes place, the abdominal epithelial replacement may involve more dynamic cell rearrangements, since the anterior (A) and posterior (P) dorsal histoblast nests expand in size and then fuse, and finally the cells migrate to cover the entire abdomen, a process that occurs within 20 h. During the replacement of the entire LEC population, local interactions between histoblasts and LECs might trigger the onset of caspase activation in LECs across the anterior/posterior (A/P) compartment border.

To test this possibility, we used a UV laser to inhibit cell division in only the posterior dorsal histoblast (PDH) nest and monitored the replacement process. As expected, most of the posterior LECs neighboring the PDH remained in the epithelium. In contrast, in the A compartment, caspase activation was frequently observed in boundary LECs, and ADH nest protrusion was observed as a result of the subsequent replacement of LECs by histoblasts (Fig. 6F). Interestingly, while both anterior and posterior LECs attached to ADH cells, we found that this contact did not frequently trigger caspase activation in posterior compartment LECs (Fig. 6G). These results suggested that the induction of caspase activation in LECs through interactions with proliferating histoblasts was restricted by the A/P developmental compartments, such that the ADHs replace the anterior LECs and the PDHs replace the posterior LECs. Thus, the A/P border must present some sort of geographical barrier or mechanism that insulates the cells from cross-border interactions, as seen in the competition between *Minute*/+ and wild-type cells in the wing disc (41, 47, 61).

DISCUSSION

Apoptosis has been implicated in tissue remodeling in development and disease. However, its regulatory mechanisms and physiological functions within the dynamic network of cellular behaviors are poorly understood. Here we report that the spatiotemporal pattern of caspase activation is controlled at the boundary between cell populations, where one population replaces the other. Our results provide evidence that the local cell cycle progression of histoblasts is associated with the initiation of nonautonomous apoptosis in the cells being replaced, and this elaborate coupling machinery could underlie the ordered replacement of cell populations.

Positional constraints affecting LEC apoptosis. In our model (Fig. 6H), LEC apoptosis at the boundary generates a patterned and orderly destruction of the larval epithelium, which enables its systematic replacement with histoblasts, a process that maintains the epithelial integrity. This model is based on the constant frequency of LEC apoptosis at the boundary with histoblasts (Fig. 2B), but at the same time we found cell-to-cell variability in the time between histoblast apposition and caspase activation in LECs. To determine whether there is any relationship between positional constraints and the time for inducing LEC apoptosis at the boundary, we categorized data for caspase activation in LECs according to the position of each LEC. We found that anterior (A) and posterior (P) LECs in the dorsal region showed similar average times required for exhibiting caspase activation, although the variability seems to be smaller for the A LECs (A LECs, 168.5 ± 86.1 min; P-LECs, 165.6 ± 141.7 min). This could explain the coordinated tissue replacement between A and P compartments during the remodeling. Since Bischoff and Cseresnyés showed that histoblasts in the P compartment move and rearrange more extensively than those in the A compartment (4), the variability of the time for P LECs could reflect histoblast-LEC interactions in the P compartment, which may be more strongly influenced by their dynamic cell rearrangements. Interestingly, some LECs which lie at the future segment boundary during the replacement showed a significantly longer time to activate caspase after the histoblast attachment (279.6 ± 131.8 min). The histoblasts which interact with these LECs at the segmental border seem to migrate in the anterior or posterior direction, perpendicular to the major directions of dorsal migration of A/P dorsal histoblasts. These LECs at the segmental border might act as a fence to canalize the dorsal migration of the histoblasts (4). Our data suggest that some mechanisms may act to prevent early apoptosis of LECs just after the histoblast attachment, or the effect of histoblast-LEC interactions could differ according to the migratory direction of histoblasts for establishing the barrier function of LECs. Unique characteristics of cells at the segment border must be involved in the restriction of the histoblast/LEC effects for caspase activation at the A/P compartment. Together, our quantitative data suggest that some sort of positional constraints might act on the timing of caspase activation during the dynamic epithelial replacement in the *Drosophila* abdomen.

are eliminated, couples histoblast proliferation with LEC apoptosis. Boundary apoptosis creates the spatiotemporal pattern of tissue removal and maintains the epithelial integrity as the histoblasts replace the LECs. Stochastic, nonboundary apoptosis also occurs at a low frequency. The A/P compartment (yellow dashed lines) is maintained between histoblasts and histoblasts/LECs during tissue remodeling. The genotypes used for the analysis were *tsh-Gal4 UAS-SCAT3*/+; *His2Av-mRFP*/+ (A to C), *hs-flp*^{122}/+; *AyGal4 UAS-SCAT3*/*UAS-PTEN* (D and E), and *tsh-Gal4 UAS-SCAT3*/+; *hh*^{PyR215}/+ (F and G).

Apoptosis during dynamic tissue remodeling in *Drosophila*. Apoptosis contributes to morphogenesis in *Drosophila*; for example, recent reports demonstrate the apoptotic death of 10 to 20% of cells during dynamic tissue rearrangements, such as in histoblasts during abdominal morphogenesis (4), in the tracheal system of the *Drosophila* embryo (2), and in the AS cells during DC (27, 65). The spatiotemporal pattern of these apoptoses seems to be stochastic. In fact, we also directly confirmed the stochastic caspase activation of AS cells during DC (Fig. 2E). Given that about 15 to 20% of LECs undergoing apoptosis were found in nonboundary areas (Fig. 2B), the stochastic apoptosis in these tissues may be functionally important in their remodeling. Considering that AS apoptosis contributes to the generation of the driving force for cell sheet movements during DC (65), the nonboundary apoptosis of LECs might also generate force to promote the movement of histoblasts. It remains unclear if stochastic apoptosis occurs as the result of the autonomous elimination of excess cells or as an accident from a mechanical force imbalance, a hypothesis that could explain the occurrence of apoptosis in dynamic cellular rearrangements (12).

We examined the frequency of caspase activation in nonboundary LECs and found that it did not differ significantly between control and proliferation-defective lines (Fig. 3J). This result suggests that a small amount of LEC apoptosis could occur autonomously or without histoblast interactions. However, the contribution of autonomous LEC death to epithelial replacement seems to be minor. In the previous study ablating histoblasts (55) and our study using proliferation-defective mutants of histoblasts (Fig. 3A to C), most of the LECs remained in the epithelia without removal. As for the mechanism of histoblast-independent death of LECs, we first consider the involvement of Ecdysone signaling. During metamorphosis, larval organ destruction depending on the Ecdysone signaling system occurs. Ninov et al. reported that in abdominal epithelial replacement, Ecdysone signaling is also necessary for both histoblast proliferation and LEC death (49). We speculate that Ecdysone signaling-dependent autonomous elimination could work to remove some LECs. Since Ecdysone signaling can trigger the expression of proapoptotic genes such as *rpr* (*reaper*) (22), it could cause LEC apoptosis by regulating the sensitivity of apoptotic signaling in some cells. Another histoblast-independent cell death mechanism may depend on hemocytes that remove some amount of LECs. During abdominal replacement, apoptotic LECs are usually engulfed by hemocytes moving beneath the epithelia (49; our unpublished data). Williams and Truman observed LEC death without contact of histoblasts, and these dying LECs did not show obvious signs of apoptosis before being engulfed by hemocytes (68). They speculated that hemocytes actively contribute to LEC death. Considering the report that hemocytes are dispensable for epithelial replacement in *Drosophila* (49), the contribution of engulfment killing might not be so significant, and further studies on the role of phagocytosis during abdominal replacement are required to settle this question.

Cell cycle-coupled behaviors of histoblasts. Previous reports have suggested mechanisms to explain the dynamic collective behaviors of histoblasts. Bischoff and Cseresnyés showed that the positions of the histoblasts depend on their cell movements, not on local cell rearrangements (4). Ninov et al. reported that histoblast nest expansion occurs mainly when the peripheral histoblasts become invasive (51). In our experiment, the inhibition of histoblast proliferation resulted in severe defects of histoblast nest expansion (Fig. 3G and 6B). The proliferation-inhibited histoblasts did not become invasive or migrate over long distances; rather, they stayed in the lateral nests at almost the same positions. Since proliferation-coupled cell migration takes place in other systems, such as in the air sac primordium in *Drosophila* (6, 58), proliferation may correlate generally with cell invasiveness and motility. Furthermore, we found that when histoblasts were arrested in the G_2 or S/G_2 phases, their interactions with the neighboring LECs did not induce LEC apoptosis (Fig. 5D and 6C). Cell cycle progression and cell cycle regulators can regulate cell fate decisions (5), and cell cycle-coupled responses to various signals such as transforming growth factor β (TGF-β), Wnt, and Notch have also recently been reported (9, 38, 69). Thus, it is plausible that cell cycle-coupled signals regulate histoblast characteristics, such as invasiveness, motility, secretion of signaling molecules, and eventually the local triggering of caspase activation in LECs, whereas the mechanisms of cell cycle-dependent signaling in the cell cycle phases or transitions will require further examination.

To determine whether the histoblast cell cycle progression or the increased number of histoblasts after cell division is more important for nonautonomous LEC apoptosis, we counted the number of histoblasts surrounding each LEC during apoptosis and found that it was 4.71 ± 1.76 (Fig. 5E), although the number of histoblasts in contact with each LEC could change dynamically during the replacement process. When histoblast proliferation was inhibited by UV laser illumination, which arrested the histoblasts in the S/G_2 phase, the number of histoblasts surrounding each LEC was 4.42 ± 1.42 (Fig. 5E), and apoptosis was severely delayed. Since the number of histoblasts surrounding each LEC did not differ significantly under the control and UV treatment conditions, the transition of cell cycle phases is likely to be a determinant for nonautonomous LEC apoptosis.

Cell competition-like interactions at different cell boundaries. Our findings suggest that there is a similarity in the interactions between LECs and histoblasts at the replacement boundary events and competitive interactions between cell populations. Local interactions, winner/loser identities, and the geographical limitations enforced at the compartment boundary during abdominal epithelial replacement are all hallmarks of cell competition (23). Moreover, Li et al. reported that cell competition in imaginal disc epithelia accompanies the oriented divisions of the cells that surround, and compensate for, the dying cells (42). Although in their study, it is unclear whether the frequency of cell division or the cell cycle phase is coupled to apoptosis, their finding also suggests that cell cycle progression is involved in the coordination of proliferation with apoptosis.

In *Drosophila*, the homolog of the human proto-oncogene *myc* (*dmyc*) regulates the experimental cell competition observed in the wing imaginal disc (10, 24, 46), and *dmyc* might also regulate the secretion of toxic factors that lead to cell competition (60). To learn if dMyc protein plays a role in abdominal cell replacement, we overexpressed *dmyc* in LECs, expecting a reversal of their fate from losers to winners. How-

ever, winner LECs did not emerge, and they did not show prolonged survival or delayed elimination (data not shown), suggesting that the alteration of the *dmyc* dosage could not determine the cell competition-like relationship between LECs and histoblasts. In the competition between germ line stem cells and cyst progenitor cells in the *Drosophila* testis, niche occupancy is determined by integrin-mediated cell adhesion (21), a completely different mechanism from the wing imaginal disc. Thus, the mechanism of cell competition-like interactions varies among the combination of cell types.

Orchestrated remodeling at the replacement boundary. We propose that the interaction boundary where histoblasts signal LECs to initiate caspase activation be called the "replacement boundary" (Fig. 6H). At this boundary, apoptosis and proliferation are coordinately executed in the two different cell populations, and tissue replacement is complete where the replacement boundary disappears, so that the size of the tissue is unaltered during its remodeling. Such a boundary-based regulation of cell replacement, which probably involves competition-like interactions, is an attractive blueprint for tissue morphogenesis and growth. Similar mechanisms may be evolutionarily conserved. For example, in the rat, when fetal liver cells are transplanted into a partially hepatectomized adult, the host cells die at the interface with the fetal transplanted cells, and the total liver mass is maintained (52). Therefore, the formation of a replacement boundary may be a common strategy for total cell replacement during development, during regeneration, and in homeostasis. The concept of the replacement boundary may be further supported by a recent finding that Decapentaplegic (Dpp) signaling mediates the invasiveness of peripheral histoblasts in their nests (51). Although how Dpp signaling is initially activated and maintained is still unknown, the resulting Dpp signal-dependent differences in cell states could influence the local interactions that couple the cell cycle progression of histoblasts with LEC apoptosis.

ACKNOWLEDGMENTS

We thank S. Hayashi, T. Tabata, B. Hay, C. Lehner, D. J. Pan, L. A. Johnston, M. Schubiger, S. Nosseli, T. Lee, the Bloomington Stock Center, and the Kyoto Stock Center (DGRC) for fly strains, H. Richardson for anti-cyclin E antibody, and J. H. Yoder for the protocol for pupal epithelial staining. We are grateful to K. Takemoto, S. Hayashi, A. Sakaue-Sawano, and Y. Nakamura for their kind support and suggestions. We thank the members in the Miura laboratory for valuable discussions, especially T. Chihara and Y. Yamaguchi for helpful advice and critically reading the manuscript.

This work was supported by grants from the Japanese Ministry of Education, Science, Sports, Culture, and Technology (to M.M. and E.K.), the Uehara Memorial Foundation (to E.K.), and the Takeda Science Foundation (to E.K.). Y.-I.N. is a research fellow of the Japan Society for the Promotion of Science.

The authors declare that they have no conflict of interest.

REFERENCES

1. **Akimoto, A., H. Wada, and S. Hayashi.** 2005. Enhancer trapping with a red fluorescent protein reporter in Drosophila. Dev. Dyn. **233:**993–997.
2. **Baer, M., et al.** 2010. The role of apoptosis in shaping the tracheal system in the Drosophila embryo. Mech. Dev. **127:**28–35.
3. **Bergmann, A., and H. Steller.** 2010. Apoptosis, stem cells, and tissue regeneration. Sci. Signal **3:**re8.
4. **Bischoff, M., and Z. Cseresnyés.** 2009. Cell rearrangements, cell divisions and cell death in a migrating epithelial sheet in the abdomen of Drosophila. Development **136:**2403–2411.
5. **Budirahardja, Y., and P. Gönczy.** 2009. Coupling the cell cycle to development. Development **136:**2861–2872.
6. **Cabernard, C., and M. Affolter.** 2005. Distinct roles for two receptor tyrosine kinases in epithelial branching morphogenesis in Drosophila. Dev. Cell **9:**831–842.
7. **Catalgol, B., et al.** 2009. The proteasome is an integral part of solar ultraviolet a radiation-induced gene expression. J. Biol. Chem. **284:**30076–30086.
8. **Chera, S., et al.** 2009. Apoptotic cells provide an unexpected source of Wnt3 signaling to drive hydra head regeneration. Dev. Cell **17:**279–289.
9. **Davidson, G., et al.** 2009. Cell cycle control of wnt receptor activation. Dev. Cell **17:**788–799.
10. **de la Cova, C., M. Abril, P. Bellosta, P. Gallant, and L. Johnston.** 2004. Drosophila myc regulates organ size by inducing cell competition. Cell **117:**107–116.
11. **Fan, Y., and A. Bergmann.** 2008. Distinct mechanisms of apoptosis-induced compensatory proliferation in proliferating and differentiating tissues in the Drosophila eye. Dev. Cell **14:**399–410.
12. **Farhadifar, R., J. Röper, B. Aigouy, S. Eaton, and F. J.ülicher.** 2007. The influence of cell mechanics, cell-cell interactions, and proliferation on epithelial packing. Curr. Biol. **17:**2095–2104.
13. **Friedl, P., and D. Gilmour.** 2009. Collective cell migration in morphogenesis, regeneration and cancer. Nat. Rev. Mol. Cell Biol. **10:**445–457.
14. **Friedl, P., Y. Hegerfeldt, and M. Tusch.** 2004. Collective cell migration in morphogenesis and cancer. Int. J. Dev. Biol. **48:**441–449.
15. **Gao, X., T. Neufeld, and D. Pan.** 2000. Drosophila PTEN regulates cell growth and proliferation through PI3K-dependent and -independent pathways. Dev. Biol. **221:**404–418.
16. **Girard, P., et al.** 2008. Inhibition of S-phase progression triggered by UVA-induced ROS does not require a functional DNA damage checkpoint response in mammalian cells. DNA Repair (Amst.) **7:**1500–1516.
17. **Hayashi, S.** 1996. A Cdc2 dependent checkpoint maintains diploidy in Drosophila. Development **122:**1051–1058.
18. **Hayashi, S., S. Hirose, T. Metcalfe, and A. Shirras.** 1993. Control of imaginal cell development by the escargot gene of Drosophila. Development **118:**105–115.
19. **Hipfner, D., and S. Cohen.** 2004. Connecting proliferation and apoptosis in development and disease. Nat. Rev. Mol. Cell Biol. **5:**805–815.
20. **Huh, J., M. Guo, and B. Hay.** 2004. Compensatory proliferation induced by cell death in the Drosophila wing disc requires activity of the apical cell death caspase Dronc in a nonapoptotic role. Curr. Biol. **14:**1262–1266.
21. **Issigonis, M., et al.** 2009. JAK-STAT signal inhibition regulates competition in the Drosophila testis stem cell niche. Science **326:**153–156.
22. **Jiang, C., A. Lamblin, H. Steller, and C. Thummel.** 2000. A steroid-triggered transcriptional hierarchy controls salivary gland cell death during Drosophila metamorphosis. Mol. Cell **5:**445–455.
23. **Johnston, L.** 2009. Competitive interactions between cells: death, growth, and geography. Science **324:**1679–1682.
24. **Johnston, L., D. Prober, B. Edgar, R. Eisenman, and P. Gallant.** 1999. Drosophila myc regulates cellular growth during development. Cell **98:**779–790.
25. **Kanuka, H., et al.** 2005. Drosophila caspase transduces Shaggy/GSK-3beta kinase activity in neural precursor development. EMBO J. **24:**3793–3806.
26. **Kassis, J.** 1994. Unusual properties of regulatory DNA from the Drosophila engrailed gene: three "pairing-sensitive" sites within a 1.6-kb region. Genetics **136:**1025–1038.
27. **Kiehart, D., C. Galbraith, K. Edwards, W. Rickoll, and R. Montague.** 2000. Multiple forces contribute to cell sheet morphogenesis for dorsal closure in Drosophila. J. Cell Biol. **149:**471–490.
28. **Knoblich, J., et al.** 1994. Cyclin E controls S phase progression and its down-regulation during Drosophila embryogenesis is required for the arrest of cell proliferation. Cell **77:**107–120.
29. **Kondo, S., N. Senoo-Matsuda, Y. Hiromi, and M. Miura.** 2006. DRONC coordinates cell death and compensatory proliferation. Mol. Cell. Biol. **26:**7258–7268.
30. **Koto, A., E. Kuranaga, and M. Miura.** 2011. Apoptosis ensures spacing pattern formation of Drosophila sensory organs. Curr. Biol. **21:**278–287.
31. **Koto, A., E. Kuranaga, and M. Miura.** 2009. Temporal regulation of Drosophila IAP1 determines caspase functions in sensory organ development. J. Cell Biol. **187:**219–231.
32. **Kumar, S.** 2007. Caspase function in programmed cell death. Cell Death Differ. **14:**32–43.
33. **Kuranaga, E., et al.** 2006. Drosophila IKK-related kinase regulates nonapoptotic function of caspases via degradation of IAPs. Cell **126:**583–596.
34. **Kuranaga, E., et al.** 2011. Apoptosis controls the speed of looping morphogenesis in Drosophila male terminalia. Development **138:**1493–1499.
35. **Kylsten, P., and R. Saint.** 1997. Imaginal tissues of Drosophila melanogaster exhibit different modes of cell proliferation control. Dev. Biol. **192:**509–522.
36. **Lai, S., and T. Lee.** 2006. Genetic mosaic with dual binary transcriptional systems in Drosophila. Nat. Neurosci. **9:**703–709.
37. **Lane, M., et al.** 1996. Dacapo, a cyclin-dependent kinase inhibitor, stops cell proliferation during Drosophila development. Cell **87:**1225–1235.
38. **Latasa, M., E. Cisneros, and J. Frade.** 2009. Cell cycle control of Notch signaling and the functional regionalization of the neuroepithelium during vertebrate neurogenesis. Int. J. Dev. Biol. **53:**895–908.

39. **Lecuit, T., and L. Le Goff.** 2007. Orchestrating size and shape during morphogenesis. Nature **450:**189–192.
40. **Lee, P., et al.** 2009. Dynamic expression of epidermal caspase 8 simulates a wound healing response. Nature **458:**519–523.
41. **Li, W., and N. Baker.** 2007. Engulfment is required for cell competition. Cell **129:**1215–1225.
42. **Li, W., A. Kale, and N. Baker.** 2009. Oriented cell division as a response to cell death and cell competition. Curr. Biol. **19:**1821–1826.
43. **Madhavan, M., and K. Madhavan.** 1980. Morphogenesis of the epidermis of adult abdomen of Drosophila. J. Embryol. Exp. Morphol. **60:**1–31.
44. **Morata, G., and P. Ripoll.** 1975. Minutes: mutants of Drosophila autonomously affecting cell division rate. Dev. Biol. **42:**211–221.
45. **Moreno, E.** 2008. Is cell competition relevant to cancer? Nat. Rev. Cancer **8:**141–147.
46. **Moreno, E., and K. Basler.** 2004. dMyc transforms cells into super-competitors. Cell **117:**117–129.
47. **Moreno, E., K. Basler, and G. Morata.** 2002. Cells compete for decapentaplegic survival factor to prevent apoptosis in Drosophila wing development. Nature **416:**755–759.
48. **Morin, X., R. Daneman, M. Zavortink, and W. Chia.** 2001. A protein trap strategy to detect GFP-tagged proteins expressed from their endogenous loci in Drosophila. Proc. Natl. Acad. Sci. U. S. A. **98:**15050–15055.
49. **Ninov, N., D. Chiarelli, and E. Martín-Blanco.** 2007. Extrinsic and intrinsic mechanisms directing epithelial cell sheet replacement during Drosophila metamorphosis. Development **134:**367–379.
50. **Ninov, N., C. Manjón, and E. Martín-Blanco.** 2009. Dynamic control of cell cycle and growth coupling by Ecdysone, EGFR, and PI3K signaling in Drosophila histoblasts. PLoS Biol. **7:**e1000079.
51. **Ninov, N., et al.** 2010. Dpp signaling directs cell motility and invasiveness during epithelial morphogenesis. Curr. Biol. **20:**513–520.
52. **Oertel, M., A. Menthena, M. Dabeva, and D. Shafritz.** 2006. Cell competition leads to a high level of normal liver reconstitution by transplanted fetal liver stem/progenitor cells. Gastroenterology **130:**507–520.
53. **Pellettieri, J., and A. Sánchez Alvarado.** 2007. Cell turnover and adult tissue homeostasis: from humans to planarians. Annu. Rev. Genet. **41:**83–105.
54. **Pérez-Garijo, A., F. Martín, and G. Morata.** 2004. Caspase inhibition during apoptosis causes abnormal signalling and developmental aberrations in Drosophila. Development **131:**5591–5598.
55. **Poodry, C.** 1975. Autonoumos and non-autonoumous cell death in the metamorphosis of the epidermis of Drosophila. Wilhelm Roux's Arch. **178:**333–336.
56. **Ryoo, H., T. Gorenc, and H. Steller.** 2004. Apoptotic cells can induce compensatory cell proliferation through the JNK and the Wingless signaling pathways. Dev. Cell **7:**491–501.
57. **Sakaue-Sawano, A., et al.** 2008. Visualizing spatiotemporal dynamics of multicellular cell-cycle progression. Cell **132:**487–498.
58. **Sato, M., and T. Kornberg.** 2002. FGF is an essential mitogen and chemoattractant for the air sacs of the drosophila tracheal system. Dev. Cell **3:**195–207.
59. **Schubiger, M., C. Carré, C. Antoniewski, and J. Truman.** 2005. Ligand-dependent de-repression via EcR/USP acts as a gate to coordinate the differentiation of sensory neurons in the Drosophila wing. Development **132:**5239–5248.
60. **Senoo-Matsuda, N., and L. Johnston.** 2007. Soluble factors mediate competitive and cooperative interactions between cells expressing different levels of Drosophila Myc. Proc. Natl. Acad. Sci. U. S. A. **104:**18543–18548.
61. **Simpson, P., and G. Morata.** 1981. Differential mitotic rates and patterns of growth in compartments in the Drosophila wing. Dev. Biol. **85:**299–308.
62. **Stern, B., G. Ried, N. Clegg, T. Grigliatti, and C. Lehner.** 1993. Genetic analysis of the Drosophila cdc2 homolog. Development **117:**219–232.
63. **Takemoto, K., et al.** 2007. Local initiation of caspase activation in Drosophila salivary gland programmed cell death in vivo. Proc. Natl. Acad. Sci. U. S. A. **104:**13367–13372.
64. **Takemoto, K., T. Nagai, A. Miyawaki, and M. Miura.** 2003. Spatio-temporal activation of caspase revealed by indicator that is insensitive to environmental effects. J. Cell Biol. **160:**235–243.
65. **Toyama, Y., X. Peralta, A. Wells, D. Kiehart, and G. Edwards.** 2008. Apoptotic force and tissue dynamics during Drosophila embryogenesis. Science **321:**1683–1686.
66. **Tseng, A., D. Adams, D. Qiu, P. Koustubhan, and M. Levin.** 2007. Apoptosis is required during early stages of tail regeneration in Xenopus laevis. Dev. Biol. **301:**62–69.
67. **Wells, B., E. Yoshida, and L. Johnston.** 2006. Compensatory proliferation in Drosophila imaginal discs requires Dronc-dependent p53 activity. Curr. Biol. **16:**1606–1615.
68. **Williams, D., and J. Truman.** 2005. Cellular mechanisms of dendrite pruning in Drosophila: insights from in vivo time-lapse of remodeling dendritic arborizing sensory neurons. Development **132:**3631–3642.
69. **Yang, Y., X. Pan, W. Lei, J. Wang, and J. Song.** 2006. Transforming growth factor-beta1 induces epithelial-to-mesenchymal transition and apoptosis via a cell cycle-dependent mechanism. Oncogene **25:**7235–7244.